ORGANIC LETTERS

2012
Vol. 14, No. 21
5456–5459

Structural Diversity of New C_{13}-Polyketides Produced by *Chaetomium mollipilium* Cultivated in the Presence of a NAD^+-Dependent Histone Deacetylase Inhibitor

Teigo Asai,*,† Shuntaro Morita,† Naoki Shirata,† Tohru Taniguchi,‡ Kenji Monde,‡ Hiroaki Sakurai,§ Tomoji Ozeki,§ and Yoshiteru Oshima*,†

Graduate School of Pharmaceutical Sciences, Tohoku University, Aoba-yama, Aoba-ku, Sendai 980-8578, Japan, Faculty of Advanced Life Science, Frontier Research Center for Post-Genome Science and Technology, Hokkaido University, Kita 21 Nishi 11, Sapporo 001-0021, Japan, and Department of Chemistry and Materials Science, Tokyo Institute of Technology, 2-12-1-H-63 O-okayama, Meguro-ku, Tokyo 152-8551, Japan

tasai@m.tohoku.ac.jp

Received September 14, 2012

ABSTRACT

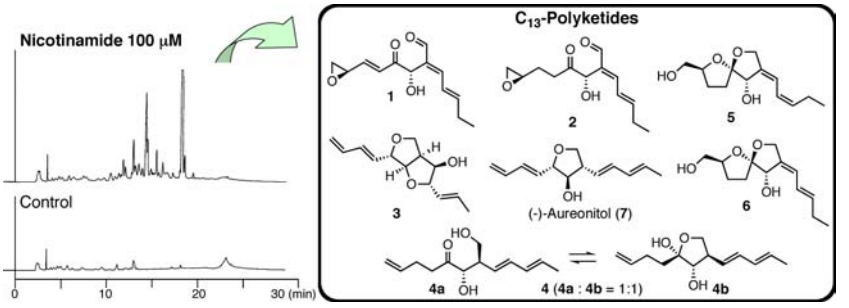

Cultivation of *Chaetomium mollipilium* with nicotinamide, a NAD^+-dependent HDAC inhibitor, stimulated its secondary metabolism, leading to the isolation of structurally diverse new C_{13}-polyketides, mollipilin A–E (1–5) as well as two known compounds (6 and 7). Spectroscopic methods, X-ray single crystal diffraction analysis, and VCD elucidated the absolute configurations of structures 1–6, and plausible biosynthetic pathways for 1–7 were proposed based on structural relationships. Mollipilins A (1) and B (2) exhibited moderate growth inhibitory effects on HCT-116 cells.

Histone deacetylases (HDACs) are an important class of enzymes capable of removing the acetyl group from ε-*N*-acetyl lysine residues in the amino-terminal tail of core histones. HDACs suppress gene expression in most cases and are crucial epigenetic factors.[1] Based on the hydrolysis mechanism, HDACs are classified into two families: Zn-(II)-dependent and NAD^+-dependent deacetylases.[2] Recent studies have shown that HDACs transcriptionally regulate fungal secondary metabolite production.[3,4] A disruption mutant of HdaA, a Zn(II)-dependent HDAC, significantly increases the expression of secondary metabolite gene clusters in *Aspergillus nidulans*, including those producing sterigmatocystin and penicillin.[3] Moreover, suberoylanilide hydroxamic acid (SAHA), which is a representative Zn(II)-dependent HDAC inhibitor, suppresses the HDAC activity in several fungi, and the increased accumulation of their metabolites has resulted in the discovery of several new compounds.[5]

We have applied this type of HDAC inhibitor, mainly suberoyl bis-hydroxamic acid (SBHA), to entomopathogenic

† Tohoku University.
‡ Hokkaido University.
§ Tokyo Institute of Technology.

(1) Ruijter, A. J. M.; Gennip, A. H. V.; Caron, H. N.; Kemp, S.; Kuilenburg, A. B. P. *Biochim. J.* **2003**, *370*, 737–749.
(2) Grozinger, C. M.; Schreiber, S. L. *Chem. Biol.* **2002**, *9*, 3–16.
(3) Shwab, E. K.; Bok, J. W.; Tribus, M.; Galehr, J.; Graessle, S.; Keller, N. P. *Eukaryot. Cell* **2007**, *6*, 1656–1664.
(4) Lee, I.; Oh, J. H.; Shwab, E. K.; Dagenais, R. T.; Andes, D.; Keller, N. P. *Fungal Genet. Biol.* **2009**, *46*, 782–790.

10.1021/ol302539s
Published on Web 10/19/2012

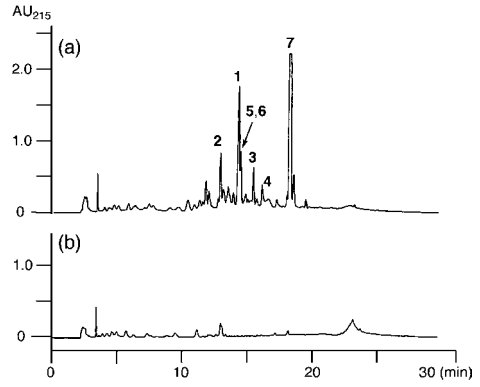

Figure 1. HPLC profiles of the EtOAc extracts of *C. mollipilium* cultivated with (a) nicotinamide 100 μM and (b) control as detected by UV absorption at 215 nm.

fungi and successfully isolated numerous novel natural products containing unprecedented carbon skeletal compounds, including tenuipyrone and indigotides C–E.[6] Although NAD^+-dependent HDACs have been identified in a number of fungi[7] and are involved in the formation and spreading of heterochromatin for transcriptional silencing,[8] a study of their effects on secondary metabolite production in fungi has yet to be reported. We hypothesized that the addition of a NAD^+-dependent HDAC inhibitor in a fungal culture medium would realize transcriptional upregulation of biosynthetic gene clusters and enhance the production of fungal secondary metabolites. Consequently, we applied three typical inhibitors (nicotinamide, sirtinol, and splitomycin)[9] to our natural product study and found that *Chaetomium mollipilium* cultivated with nicotinamide (100 μM) showed a notable change in the secondary metabolites (Figure 1). Five new C_{13}-polyketides, mollipilin A–E (**1**–**5**), as well as known spiroketal **6** (named as mollipilin F) and (−)-aureonitol (**7**) were isolated. Herein we discuss the structures of **1**–**5** and the absolute stereochemistry of **6** as well as their plausible biosynthetic relationship and cell growth inhibitory activity.

(5) (a) Williams, R. B.; Henrikson, J. C.; Hoover, A. R.; Lee, A. E.; Cichewicz, R. H. *Org. Biomol. Chem.* **2008**, *7*, 1895–1897. (b) Henrikson, J. C.; Hoover, A. R.; Joyner, P. M.; Cichewicz, R. H. *Org. Biomol. Chem.* **2009**, *7*, 435–438.

(6) (a) Asai, T.; Yamamoto, T.; Oshima, Y. *Tetrahedron Lett.* **2011**, *52*, 7042–7045. (b) Asai, T.; Dan, L.; Obara, Y.; Taniguchi, T.; Monde, K.; Yamashita, K.; Oshima, Y. *Tetrahedron Lett.* **2012**, *53*, 2239–2243. (c) Asai, T.; Chung, Y. M.; Sakurai, H.; Ozeki, T.; Chang, F. R.; Yamashita, K.; Oshima, Y. *Org. Lett.* **2012**, *54*, 513–515. (d) Asai, T.; Yamamoto, T.; Oshima, Y. *Org. Lett.* **2012**, *54*, 2006–2009.

(7) (a) Graessle, S.; Dangl, M.; Haas, H.; Mair, K.; Trojer, P.; Brandtner, E. M.; Walton, J. D.; Loidl, P.; Brosch, G. *Biochim. Biophys. Acta* **2000**, *1492*, 120–126. (b) Trojer, P.; Brandtner, E. M.; Brosch, G.; Loidl, P.; Galehr, J.; Linzmaier, R.; Haas, H.; Mair, K.; Tribus, M.; Graessle, S. *Nucleic Acids Res.* **2003**, *31*, 3971–3981.

(8) Denu, J. M. *Curr. Opin. Chem. Biol.* **2005**, *9*, 431–440.

(9) HPLC analyses of the extracts obtained from the fungal culture broths using sirtinol or splitomycin showed that no extract had distinct enhancement of the secondary metabolite production. Moreover, it showed that major constituents in the extracts were degradation and hydroxylation products of sirtinol or splitomycin, suggesting that the two inhibitors were unstable in the culture media of fungi. Therefore, the two inhibitors seemed to be unsuitable for the experiments.

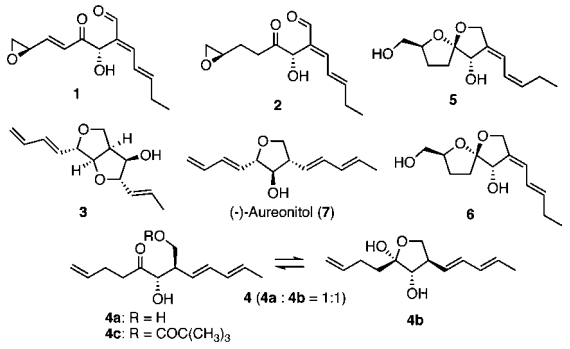

Figure 2. Structures of **1**–**7**.

C. mollipilium was cultivated in a YM liquid medium with 100 μM nicotinamide for 16 days at 25 °C (Supporting Information). The culture medium (13 L) was extracted twice with ethyl acetate. The ethyl acetate extract (1.4 g) was separated by Sephadex LH-20, silica gel column chromatography, and reversed-phase HPLC to afford diverse C13-polyketides, mollipilin A (**1**, 17.3 mg), B (**2**, 13.7 mg), C (**3**, 5.7 mg), D (**4**, 5.5 mg), E (**5**, 2.7 mg), F (**6**, 14.6 mg), and (−)-aureonitol (**7**, 488 mg) (Figure 2).

The HREIMS of mollipilin A (**1**) at m/z 236.1049 $[M]^+$ (calcd: m/z 236.1049) suggested that the molecular formula was $C_{13}H_{16}O_4$, which required six degrees of unsaturation. The IR spectrum (3445, 1698, and 1674 cm^{-1}) indicated the presence of a hydroxy group and two α,β-unsaturated carbonyl groups. The ^{13}C NMR and DEPT spectra showed the presence of one keto carbonyl, one aldehyde, one quaternary sp^2 carbon, five tertiary sp^2 carbons, two oxymethines, one oxymethylene, one methylene, and one methyl group (Table S1). The ^1H and ^{13}C NMR and HMQC spectra indicated the presence of an epoxide function based on resonance signals at δ_C 50.4 (C-11) and 49.4 (C-12) and δ_H 3.40 (ddd, J = 7.3, 5.0, 2.2 Hz, H-11), 3.06 (dd, J = 5.5, 5.0 Hz, Ha-12), and 2.69 (dd, J = 5.5, 2.2 Hz, Hb-12). The ^1H–^1H COSY spectrum exhibited sequential correlations from H_3-1 to H-5 and H-9 to H_2-12, while the HMBC correlations from H-9 and H-10 to C-8 carbonyl implied the presence of a 9-en-8-one function (Figure 3). In addition, the long-range correlations of H-4/C-6, H-5/C-13, and H-7/C-6, C-8 suggested C-5–C-6–C-13 and C-6–C-7–C-8 linkages (Figure 3), and the large coupling constants of H-3/H-4 (15.6 Hz) and H-9/H-10 (15.8 Hz) indicated that C-3/C-4 and C-9/C-10 olefins had *trans* geometries (Table S1). The 5*E* configuration from the NOE of H-5/H-13 confirmed the planar structure of **1** (Figure 3).

The ^1H and ^{13}C NMR spectra of mollipilin B (**2**), $C_{13}H_{18}O_4$ [HREIMS: m/z 238.1194 $[M]^+$ (calcd: m/z 238.1205)], agreed well with those of **1**, except **2** had two additional methylene signals and lacked the signals assigned to the C-9/C-10 *trans*-olefin in **1** (Table S1). These observations suggested that the C-9/C-10 double bond in **1** was reduced to methylenes in **2**, which was consistent with the strong IR band at 1718 cm^{-1} due to a saturated

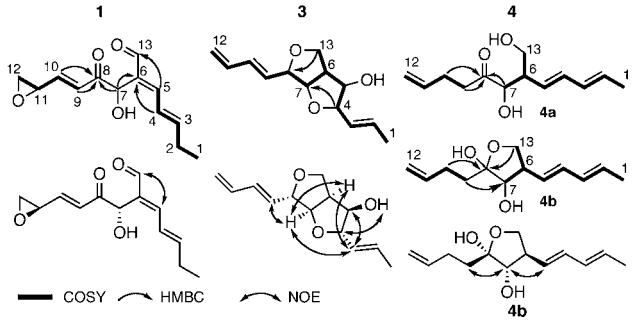

Figure 3. Key ^{1}H−^{1}H COSY, HMBC, and NOE correlations of **1**, **3**, and **4**.

carbonyl group. Analysis of the COSY and HMBC spectra showed that **2** was a 9,10-dihydro derivative of **1**.

To determine the absolute stereochemistries at C-7 and C-11 in **1**, the VCD method using DFT calculations was applied. The experimental IR and VCD spectra of **1** measured in $CDCl_3$ agreed well with the calculated spectra for 7*S*,11*S*- and 7*S*,11*R*-**1** (Figure 4), suggesting that **1** had a 7*S* configuration. Unfortunately, the VCD experiments could not elucidate the C-11 configuration because the calculated spectra of the two isomers were almost identical (Figure 4). Treatment of **1** or **2** with 2,4-dinitrophenylhydrazine yielded corresponding hydrazone **1a** or **2a**, which could be converted into the (*S*)- and (*R*)-MTPA esters (**1b**, **1c**, **2b**, and **2c**), respectively. By comparing the $\Delta\delta_{(S-R)}$ values with those of **1**, the absolute stereochemistry at C-7 in **2** was determined to be *S* (Scheme S1). Moreover, crystallized **2a**, which was supplied for an X-ray analysis study, confirmed that the absolute stereochemistry at C-11 was *R* (Figure 5), and the biosynthetic relationship between **1** and **2** implied that **1** also had an 11*R* configuration.

The molecular formula of mollipilin C (**3**) was $C_{13}H_{18}O_3$ [HREIMS: *m*/*z* 222.1226 $[M]^+$ (calcd: *m*/*z* 222.1256)],

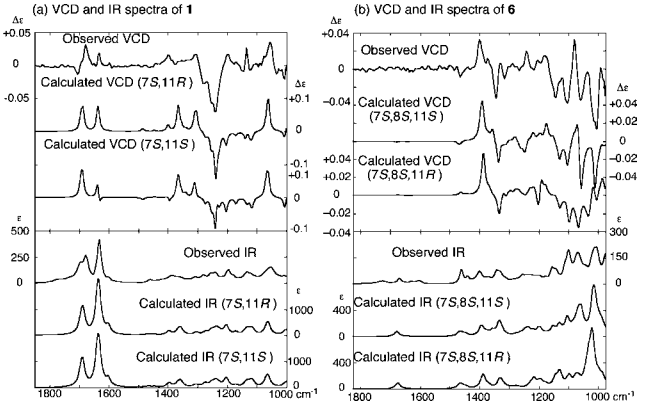

Figure 4. Comparison of IR (lower flame) and VCD (upper flame) spectra: (a) observed for **1** with those of calculated for 7*S*,11*R*- and 7*S*,11*S*-**1**; (b) observed for **6** with those of calculated for 7*S*,8*S*,11*S*- and 7*S*,8*S*,11*R*-**6**.

which required five degrees of unsaturation. The ^{1}H NMR, ^{13}C NMR, and HMQC spectra showed the presence of an exo-olefin (C-11/C-12) and two trans-olefins (C-2/C-3 and C-9/C-10) (Table S2). The above functionality accounted for 3 of the 5 degrees of unsaturation, suggesting **3** possessed a bicyclic core. In addition, the ^{13}C NMR and DEPT spectra exhibited signals for four oxymethines, one oxymethylene, one methine, and one methyl. The analysis of the ^{1}H−^{1}H COSY spectrum supported the carbon sequence in the molecule (Figure 3). The HMBC correlations of H_2-13/C-8 and H-4/C-7 revealed that the connectivity of C-8−C-13 and C-4−C-7 was through ether bonds, indicating the presence of hexahydrofuro[3,4-*b*]furan (Figure 3), and the molecular formula indicated the presence of a C-5 hydroxy group. 1D-NOE experiments elucidated the relative stereochemistry of the bicyclic core of **3**. The NOE of H-6/H-7 showed that the two tetrahydrofuran rings were fused in the *cis* configuration (Figure 3). Moreover, the NOEs (H-3/H-5, H-6, H-7, H-4/5- OH, and H-7/H-9) unequivocally defined the remaining relative stereochemistries (Figure 3), and the advanced Mosher method confirmed that the absolute stereochemistry at C-5 was *R* (Figure S1, Table S6).

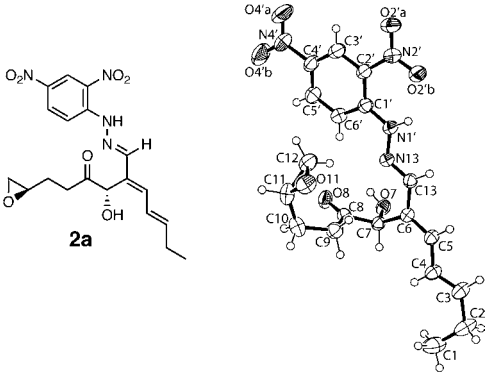

Figure 5. Structure and ORTEP stereo diagram of **2a**.

The HREIMS of **4** showed an ion peak at *m*/*z* 224.1416 ($C_{13}H_{20}O_3$, calcd: *m*/*z* 224.1412). The ^{13}C NMR assisted by HMQC spectra displayed 26 signals, including one keto carbonyl, ten tertiary sp^2 carbons, two secondary sp^2 carbons, one acetal carbon, two oxymethines, two oxymethylenes, two methines, four methylenes, and two methyls. Analyses of the ^{1}H−^{1}H COSY and HMBC spectra suggested two structures, **4a** and **4b** (Figure 3). Treatment of **4** with pivaloyl chloride afforded **4c** as a single product [HREIMS: *m*/*z* 308.1974 $[M]^+$ (calcd for $C_{18}H_{28}O_4$ 308.1988)]. The ^{1}H NMR spectrum of **4c** agreed well with that of **4a** except for the presence of a methyl signal due to the pivaloyl ester and the downfield shift of the H_2-13 signals, indicating that **4c** was the 13-*O*-pivaloylated derivative of **4a** (Figure 2). This observation confirms that **4** was an equilibrium mixture of **4a** and **4b**. The NOEs of H-7/H-5 and H_2-9 in **4b** determined the relative configurations at C-6, C-7, and C-8, and applying the advanced Mosher method to **4c** indicated that the absolute stereochemistry at C-7 was *S* (Figure S1, Table S7).

Scheme 1. Plausible Biosynthetic Relationship among the Isolated Polyketides (**1**–**7**)

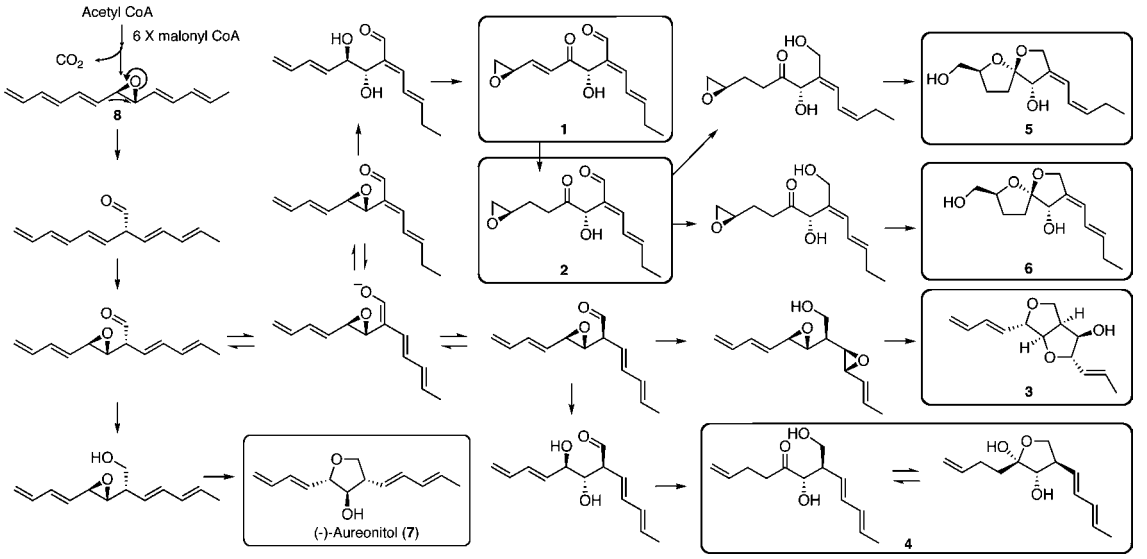

Compounds **5** and **6** had the same molecular formula $C_{13}H_{20}O_4$, and the analyses of 1D and 2D NMR showed that they were geometric isomers at the C-3/C-4 double bond (Figure S2, Table S4). A comparative study of the ^1H and ^{13}C NMR spectra with the reported data further identified **6** as 3-hydroxymethyl-8*Z*-(2′*E*-pentenyliden)-2,6-dioxaspiro[4.4]nonanol-9 (Table S4).[10] The NOEs of H-7/H_2-9 suggested **6** had a 7*S**,8*S** relative configuration (Figure S3), and the advanced Mosher method for 12-*O*-pivaloylated derivative **6a** substantiated the 7*S* configuration in **6** (Figure S1, Table S8). Although the relative stereochemistry of **6** was proposed as 7*S**,8*S**,11*R** from its NMR data,[9] stereomodeling suggested it was difficult to determine the relative stereochemistry at C-11 from NMR analysis. Consequently, a VCD study was conducted to clarify the absolute configuration at C-11 and the absolute stereochemistry of the molecule. The experimental VCD spectrum agreed well with the spectrum of the 7*S*,8*S*,11*S* isomer rather than that of 7*S*,8*S*,11*R* (Figure 4). Based on their biosynthetic relationship, **5** and **6** had the same stereochemistry. Therefore, the structures of **5** and **6** were determined as shown in Figure 2.

The cell growth inhibitory activities of polyketides **1**–**7** were evaluated in human HCT 116 cells. Mollipilin A (**1**) and B (**2**) exhibited moderate inhibitory effects on the cell growth with GI_{50} values of 1.8 and 3.7 μM, respectively. The Western blot with an antibody against acetylated histone H4 showed that nicotinamide treatment of *C. mollipilium* induced hyperacetylated histone H4 in a dose dependent manner (Figure S3). In our study of *C. mollipilium*, nicotinamide significantly affected its secondary metabolite production at concentrations of 50 and 100 μM, while the influence of 10 μM was less than that of 100 μM (data not shown). Additionally, employing isonicotinamide (100 μM), an analog of nicotinamide without NAD^+-dependent HDAC inhibitory activity, did not affect secondary metabolite production. These observations suggested that the HDAC inhibitory activity of nicotinamide was correlated with secondary metabolite production.

In this study, we demonstrated that the addition of nicotinamide to the culture medium of *C. mollipilium* significantly stimulated secondary metabolite production. A previous feeding experiment suggested a biosynthetic route of **7** from linear C_{13}-polyene **8** via an epoxide rearrangement.[11] Our findings herein, which were based on structural considerations, also indicated that **1**–**6** were biosynthesized from **8** (Scheme 1). The structural diversity in the C_{13}-polyenes was realized by an epoxide rearrangement of **8** followed by tautomerization, sequential oxidations, and rearrangements. This study is the first to demonstrate that a NAD^+-dependent HDAC inhibitor can effectively explore novel fungal secondary metabolites.

Acknowledgment. This work was supported in part by a Grant-in-Aid for Scientific Research (Nos. 23710248 and 23590582) from the Ministry of Education, Science, Sports and Culture of Japan; A-STEP (FS-stage) (No. AS231Z01347G) from Japan Science and Technology Agency (JST); the Uehara Memorial Foundation; and the Japan Association for Chemical Innovation.

Supporting Information Available. Tables, figures, schemes, experimental methods, NMR spectra of new compounds, and the cif file for the 2,4-dinitrophenylhydrazone derivative of mollipilin B (**2a**). This material is available free of charge via the Internet at http://pubs.acs.org.

The authors declare no competing financial interest.

(10) Abraham, W. R.; Arfmann, H. A. *Phytochemistry* **1992**, *31*, 2405–2408.

(11) Saito, M.; Seto, H.; Yonehara, H. *Agric. Biol. Chem.* **1983**, *47*, 2935–2937.